THERMAL CHARACTERISATION OF PARALLEL-RUNNING EMBEDDED COOLING LAYERS WITH NEGLIGIBLE THERMAL INTERFACIAL RESISTANCE FOR SINGLE DIRECTIONAL HEAT EXTRACTION

Dirker J.* and Meyer J.P.
Author for correspondence
Department of Mechanical and Aeronautical Engineering,
University of Pretoria,
Pretoria, 0002,
South Africa,
E-mail: jaco.dirker@up.ac.za

ABSTRACT

Embedded solid-state cooling layers which have relatively high thermal conductivity in terms of the heat-generating mediums into which it is introduced, presents itself as a viable passive method of reducing peak operating temperatures in, for instance, integrated power electronic and other applications where an increase in power density is of interest. The thermal performance of such a bi-material cooling method is dependent on geometric, material property and thermal interfacial parameters. This paper reports on the influence of five such identified parameters, as obtained via a numerical study. Single-directional heat extraction from a rectangular solid-state volume was considered and the thermal performance which can be obtained for such a boundary condition is described.

INTRODUCTION

A shift towards the modular integration of power electronics, resulting in increased power and loss densities [1], have necessitated the development of more effective cooling methods to reduce peak operating temperatures in such applications [2,3]. Due to low thermal conductivities associated with the outer material layers of these integrated power electronic modules [2,3], surface cooling on its own is no longer sufficient as the materials themselves act as major thermal barriers [4]. Internal heat transfer augmentation of these solid-state heat-generating volumes via the creation of low thermal resistance paths to surface regions has become crucial. Through this, restrictions placed upon future development by thermal issues may be made less critical due to the fact that components can be operated at higher power densities and at relatively lower peak temperatures. Solid state conductive cooling, being a passive cooling scheme and not being dependent on other support systems, exhibits reliability and volumetric advantages. Even though conductive heat transfer may be orders lower than heat transfer associated with convection or evaporation, its reliability aspect justifies in-depth investigations into cooling methods using this heat transfer mode.

Conductive cooling of heat-generating volumes has been approached by other researchers as a volume- or area-to-point heat transfer problem [5]. Thermal tree theories have been developed to describe the distribution of low thermal resistant paths and heat transfer has been optimised for different thermal tree structures [6-8].

Even though thermal tree schemes present optimised heat transfer performance, it requires complex geometric layouts which at small dimensional scales can lead to high manufacturing costs. In passive power electronic modules, which typically have inductive, capacitive and transformative functions, restrictions imposed by the electromagnetic fields, dictates that only parallel-running internal embedded solid geometries can be con-

NOMENCLATURE

α_{ZY}	[-]	$y-z$ view aspect ratio of rectangular region between two adjacent cooling layers
C_{GTP}	[m^{3}K/W]	Coefficient dependent on geometric, thermal and material property values
$E_{\%}$	[%]	Allowable volumetric heat generation density increase
k	[W/mK]	Thermal conductivity
$\dot{q}'''$	[W/m^3]	Volumetric heat generation density
R	[m^{2}K/W]	Interfacial thermal resistance
T	[K]	Temperature
x	[m]	Cartesian axis direction
y	[m]	Cartesian axis direction
z	[m]	Cartesian axis direction

Special characters

α	[-]	Volume fraction ratio
$\mathcal{A}$	[m]	Half centre-to-centre offset distance between neighbouring cooling inserts in the x direction
$\mathcal{B}$	[m]	Half centre-to-centre offset distance between neighbouring cooling inserts in the y direction
b	[m]	Half y directional dimension of rectangular cooling insert
ε	[-]	Relative $E_{\%}$ value in terms of maximum $E_{\%}$
γ	[-]	Ratio between thermal conductivities of cooling insert and the heat-generating medium
$\mathcal{Z}$	[m]	Half z directional dimension of rectangular cooling insert

Subscripts

C	Cooling layer
eff	Volumetric effective expression
ext	External: Towards external heat sink
int	Internal: Between cooling and heat-generating layers
M	Heat generating medium
max	Maximum
0	Ambient or reference

sidered. Such layouts, when placed in-line with magnetic field lines reduces the interference a cooling insert may have on magnetic and electric field distribution. Three-dimensional thermal path networks are thus not suitable for such applications

In a previous investigation [9], the thermal performance of a grid of discrete parallel-running rectangular solid inserts were studied and geometrically optimised in terms of fixed volume use. At the dimensional scale of interest in power electronics and electronics cooling, it was found that the geometric shape of embedded cooling inserts has a diminishing influence on thermal performance and that the fraction of volume occupied by the cooling system plays a much more dominant role [10]. With this in mind it may be appreciated that from an economic and manufacturing point of view, continuous cooling layers provides a more practical embedded conductive cooling configuration. This paper focuses on thermal characterisation of cooling layers and aims to provide some information on thermal cooling performance.

EXTERNAL BOUNDARY CONDITIONS

When considering a general rectangular three-dimensional heat-generating solid, three main external boundary conditions types can be considered, namely heat transfer to the surroundings in a singular Cartesian direction with adiabatic conditions for other directional external surface sets, orthogonal bi-directional heat transfer to the surroundings with the other external direction being adiabatic, and a case with tri-directional heat transfer to the surroundings as represented in Figure 1.

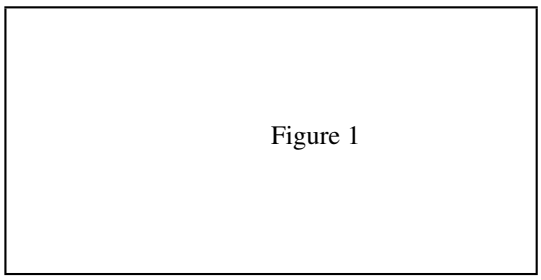

Figure 1. Three external boundary condition types

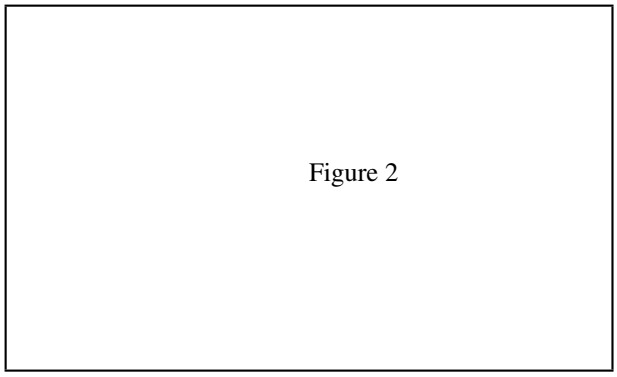

Figure 2. Single-directional and bi-directional heat extraction models

Practically, this can be interpreted as cases where the location of external surface cooling, such as heat sinks, allows for cooling in one, two, or three orthogonal Cartesian directions. In the current investigation a single-directional boundary condition is considered, representing cases where external cooling, for instance heat sinks, are mounted on one set of opposite sides of a rectangular heat-generating component. In Figure 2 an embedded layered cooling scheme, operated with a single-directional heat extraction boundary condition, is shown in contrast to a possible bi-directional heat extraction boundary condition configuration.

The representation depicts a composite heat-generating solid, which contains alternating heat-generating and cooling layers. The dimension of the composite rectangular solid in the x and z directions is defined as $2\mathcal{A}$ and $2\mathcal{Z}$ respectively. In the y direction, cooling layers are located at a constant centre-to-centre offset distances of $2\mathcal{B}$, with each layer having a thickness of $2b$. The thermal conductivities of the heat-generating medium and cooling layer material are defined as k_M [W/mK] and k_C [W/mK] respectively. Uniform heat generation density within heat-generating layers is defined as [W/m^3].

Uniform internal interfacial thermal resistance between the heat-generating layers and cooling layers are defined as R_{int} [m^{2}K/W], while external thermal resistance, R_{ext} [m^{2}K/W], are defined on external surfaces where heat transfer to the surroundings are permitted. All other external surfaces where heat transfer to the surroundings is not permitted are defined as being adiabatic.

In the single-directional heat extraction case, heat transfer is only permitted towards the surroundings in the positive and negative z directions. In the resultant model problem, no heat transfer is permitted in the y direction. The surroundings are defined to be at a constant uniform temperature of T_0. This temperature can be used to describe for instance the average temperature of an external heat sink or heat spreading plate.

Due to the repetitive internal layered structure, the symmetric nature of the model in the z direction, and the fact that heat extraction to the surrounding in the y direction is not permitted it is possible to define smaller representative domains, with which thermal calculations can be done.

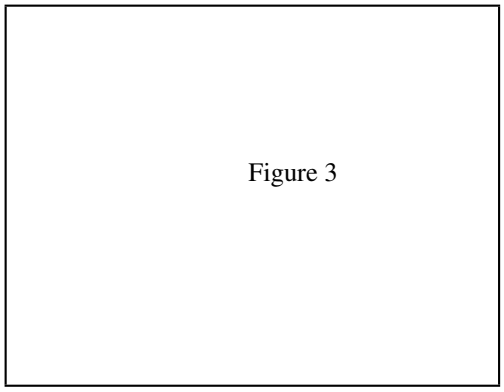

Figure 3. Representative domains used for thermal modelling

For a single directional heat extraction boundary type, a two-dimensional representative model is sufficient as no temperature gradients are present in the x direction. A schematic diagram is given in Figure 3. In agreement with Figure 2, the dimensions of representative domain in the y and z directions were defined to be $\mathcal{B}$ and $\mathcal{Z}$ respectively. External thermal resistance was defined to be on the positive z face of both the heat-generating and cooling layers. All other faces where defined to be adiabatic. Due to the symmetric nature of the model problem, the location of the peak temperature, $T_{\max}$, in the representative domain corresponds to a position in the heat-generating medium halfway between two adjacent cooling layers and midway along the z-directional length of the rectangular volume.

NUMERICAL METHOD

A numerical solution approach was followed as pure analytical solutions for the thermal governing equations proved to be elusive. Due to the anticipated large number of case study investigations, which were required to thermally characterise the model problem, problem specific algorithms were developed. With these algorithms the simulations processes could be automated, eliminating the time- consuming pre-processing stages required in commercial numerical software packages.

It was the purpose of the developed algorithms to calculate the temperature fields within the domains for different input values of $\mathcal{B}$, $\mathcal{Z}$, b, k_M, k_C, R_{int}, R_{ext}, T_0, and $\dot{q}_M$. In order to use a numerical solution method, the representative domain was decomposed into hexahedral elements defined around nodal points. Uniformly spaced grid points (nodes) where defined in such a way that no grid points fell directly onto faces where heat transfer occurred.

A vertex centred finite volume numeric method was followed to solve for the steady state temperature field by means of a fully implicit matrix approach. With this method, the governing differential equation, is discretised for rectangular three-dimensional control volumes and the variable being solved for (in this case temperature) is expressed in terms of variable values of neighbouring control volumes by a single linear type equation. For a system with N number of grid points, N number of equations is required from which a N-by-N matrix can be constructed.

LU-decomposition of the constructed matrix was employed, where after back and forward substitution was used to obtain the temperature solution. Due to the fact that the model problem was two-dimensional in nature, no node-renumbering scheme, such as the reverse Cuthill-McKee algorithm, could be employed to speed up solution times.

Validation of Numerical Models

For the developed problem-specific algorithm, it was found that mesh-independent temperature solutions were obtained when ten or more nodes are used in the y and z Cartesian mesh directions. When the number of nodes is doubled, less than 1% difference in the calculated temperature solutions was present. All subsequent simulation work was performed with ten nodes in the y and z Cartesian directions.

The problem-specific numerical model was validated numerically with the use of the commercially available computational package, STAR-CD. A comparison of the temperature distributions obtained for an arbitrary case from the STAR-CD simulation result and that of the two-dimensional numerical model is shown in Figure 4 along a nodal line in the y direction. It was found that temperature values agreed within 0.1 °C of each other. In addition to excellent numerical agreement, in a previous experimental study [4], it was found that the two-dimensional model predicted relative thermal behaviour, for a single-directional surface heat extraction case, within 5%.

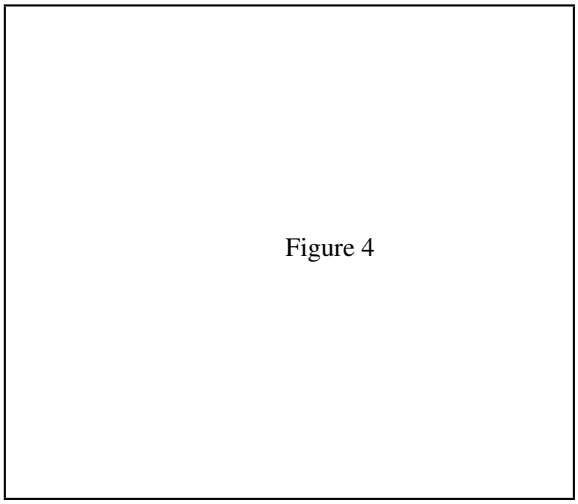

Figure 4. Temperature distribution comparison with numerical STAR-CD results for the two-dimensional model

PROCESSING OF RESULTS

The cooling ability of a particular set-up can be expressed by means of a thermo-geometric coefficient, C_{GTP} [m^{3}K/W]. This coefficient can be used to relate the maximum temperature rise within the representative domain (in terms of the ambient temperature), $\Delta T_{\max}$ [°C] to the volumetric heat generation density:

$$\Delta T_{\max} = \dot{q}'''_M / C_{GTP} = T_{\max} - T_0 \tag{1}$$

For a homogeneous volume consisting of only heat-generating material, C_{GTP} can be expressed as:

$$C_{GTP} = \left(\frac{z^2}{2k_M} + ZR_{ext} \right)^{-1} \tag{2}$$

For a bi-material case where cooling layers are also present, the value of C_{GTP} can be obtained via the developed numerical model. The effective volumetric heat-generation density increase at a fixed peak temperature, $E_{\%,eff}$ [%], can be defined as the percentage increase in the overall heat generation density which a composite volume consisting of both heat-generating and cooling insert materials can accommodate above that of a homogeneous heat-generating material while maintaining the original

peak temperature. When a is used as the volume fraction occupied by cooling, equation (1) can be utilised and $E_{\%,eff}$ can be express as follows:

$$E_{\%,eff} = 100\,(1-\alpha)\left(\left.\frac{C_{GTP,\,\text{with cooling}}}{C_{GTP,\,\text{no cooling}}}\right|_{\Delta T_{\max}=\text{Const}} - 1\right) \quad (3)$$

TRENDS AND RESULTS

It was found that for cases where no internal or external thermal interfacial resistances are present, $E_{\%,eff}$ is not dependent on the absolute magnitudes of the thermal conductivities, but rather by the thermal conductivity ratio, γ [ ], defined as:

$$\gamma = k_C/k_M \quad (4)$$

Similary, so does only the slenderness ratio of the two-dimensional region between the mid-plane surfaces of neighbouring cooling layers, a_{ZY}, influence $E_{\%,eff}$, and not the absolute magnitude of $\mathcal{B}$ and $\mathcal{Z}$. Here this slenderness ratio is defined as follows:

$$a_{ZY} = \mathcal{Z}/\mathcal{B} \quad (5)$$

In Figure 5 to Figure 7 the impact of these two non-dimensional ratios on $E_{\%,eff}$ is demonstrated for a values of 0.1, 0.2, and 0.5 (10%, 20% and 50% of volume used for cooling purposes). From the graphs it can clearly be seen that an increase in a or γ results in higher $E_{\%,eff}$ values.

As is shown, the presence of heat extraction cooling layers can dramatically increase the thermal performance of a heat generating volume. This can be demonstrated by hand of an example where aluminium nitride cooling layers with a thermal conductivity of approximately 170 W/mK is embedded into ferrite (a material commonly used in power electronic passives) with a thermal conductivity of approximately 5 W/mK. With a thermal conductivity ratio, γ = 34, it is predicted that for a case where 10% of the volume is occupied by cooling that the thermal performance of the structure can be increased by between 80% and 300% depending on the a_{ZY} geometric ratio.

It was found that for all a and γ combinations $E_{\%,eff}$ approaches an upper limit asymptote, $E_{\%,eff,\max}$, as the number of cooling layers are increased and their thickness reduced in proportion (while maintaining a constant α). An increase in a_{ZY}) indicates thinner cooling and heat-generating layers. The maximum $E_{\%,eff}$ value was found to be directly proportional to a and γ and can be expressed as follows:

$$E_{\%,eff,\max} = 100\alpha\gamma \quad (6)$$

When, however cooling layers offset distances are excessively large, the thermal performance of a component can in actual fact

Figure 5

Figure 5. Influence of a_{ZY} and γ on $E_{\%,eff}$ for no thermal interfacial resistances with α = 0.1

Figure 6

Figure 6. Influence of a_{ZY} and γ on $E_{\%,eff}$ for no thermal interfacial resistances with α = 0.2

Figure 7

Figure 7. Influence of a_{ZY} and γ on $E_{\%,eff}$ for no thermal interfacial resistances with α = 0.5

also be deteriorated by the inclusion of cooling layers. The lower limit of $E_{\%,eff}$ is dependent only upon a and can be expressed as:

$$E_{\%,eff,\min} = -100\alpha \tag{7}$$

Equation (6) gives the ultimate maximum value with which heat generation density can be increased for a fixed volume fraction and relative cooling material thermal conductivity. Practically this maximum value can be approached by reducing the thickness of the alternating heating and cooling layers.

It was found however that this equation is only valid for calculating $E_{\%,eff,\max}$ values once the critical cooling layer thickness and offset condition is reached. The equation can thus not be used with accuracy to compare different a and γ cases if this is not true. The slenderness of the volume between two neighbouring cooling layers in the z directions can be used to describe relative layer thickness. For this, the ratio a_{ZY} defined in equation (5) can be utilised to describe critical relative conditions, which will be denoted here by a^*_{ZY}. Critical conditions are assumed to have been reached once the following conditions is true:

$$E_{\%,eff} \geq 0.99E_{\%,eff,\max} \tag{8}$$

Once this condition is reached, no significant additional thermal performance increase is obtained by further increasing the number of cooling layers and reducing their thickness in proportion. The dependence of a^*_{ZY} on α and γ is demonstrated in Figure 8 for cases where no thermal interfacial resistance is present.

From this graph it can be observed that a^*_{ZY} reaches a maximum at α = 0.5 and that a^*_{ZY} increases as γ is increased (higher a^*_{ZY} values represent conditions with thinner cooling layers). Practically this means that in relation, utilising cooling layers with higher thermal conductivities would require more, and thinner cooling layers to reach maximum $E_{\%,eff}$ values, than would have been the case when using lower thermal conductivity layers. Even though higher thermal conductivity layers exhibit higher maximum $E_{\%,eff}$ values, its ability to reach such conditions becomes very dependent upon the practical manufacturing limit of producing cooling layers which are thin enough.

For cases where critical conditions for layer thickness and offset distances have not been reached, $E_{\%,eff}$ values below that of $E_{\%,eff,\max}$ are exhibited by the system. The effective thermal performance increase can then be expressed as follows:

$$E_{\%,eff} = \varepsilon E_{\%,eff,\max} = 100\alpha\varepsilon\gamma \tag{9}$$

Coefficient ε can be seen as a proportional fraction between the achievable $E_{\%,eff}$ for a particular cooling layer thickness and offset distance condition, and the ultimate maximum $E_{\%,eff}$ value expressed by equation (6) when critical layer conditions are reached.

Figure 8

Figure 8. Critical a_{ZY} values for different α and γ conditions for a single-directional heat extraction boundary condition.

Figure 9 demonstrates the dependence of ε upon α, γ and the ratio a_{ZY}/a^*_{ZY}. The ratio a_{ZY}/a^*_{ZY} serves as an indication of relative layer-thickness and offset-distance conditions in terms of the critical layer thickness and offset distance condition. From the graph it can be observed that ε is not significantly impacted by α for γ values above 30. Also, very constant ε values are obtained for a wide range of γ values and it was found that for a_{ZY}/a^*_{ZY} ratios of 0.5, 0.2, and 0.1, ε values in the regions of 0.95, 0.8 and 0.5 respectively are obtained. This corresponds to $E_{\%,eff}$ values of 95%, 80% and 50% of the ultimate $E_{\%,eff}$ values predicted by equation (6). As is expected, the thermal performance increase becomes less as layering conditions expressed by a_{ZY}, are further removed from critical layering conditions.

In conjunction with equation (9) the information contained in Figure 9, can be used to determine the $E_{\%,eff}$ values for a large range of geometric and material property values applicable to a single-directional heat-extraction case.

With the information given in Figure 8 and Figure 9 the thermal advantage, and thus the factor by which effective heat generation density can be increased with due to the presence of embedded cooling layers, can be determined. Even though the trends described here are valid only for cases where thermal interfacial resistance values are negligibly small, it serves as a valuable tool in designing and predicting the thermal performance of an embedded cooling layer scheme.

CONDITIONS WITH THERMAL INTERFACIAL RESISTANCE

When thermal interfacial resistance, either internally between heat generating and cooling layers; or externally between the composite heat-generating bi-material component and external cooling components are no longer negligible, the thermal performance increase of an embedded cooling layer scheme is reduced.

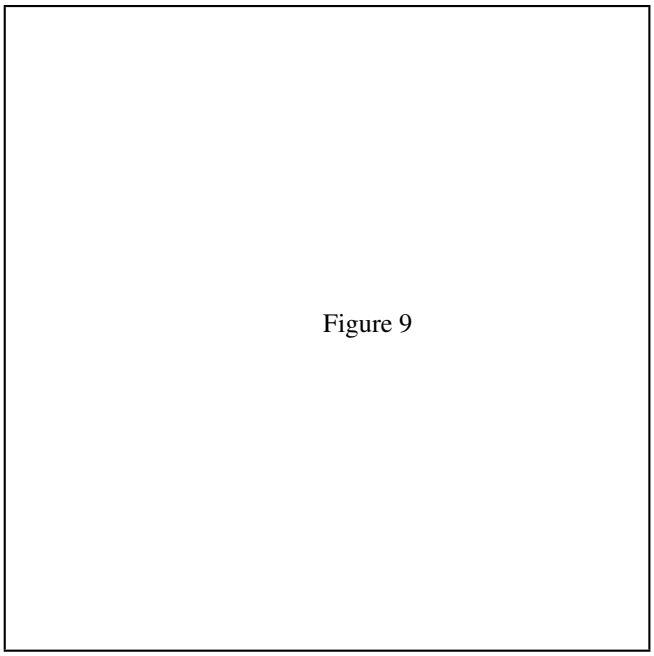

Figure 9. Numerically obtained ε values for cases with no thermal interfacial resistances when critical layer thickness is not reached.

It was found that at small dimensional scales in the order of 10 mm or less for $\mathcal{Z}$, interfacial resistance values of 0.0001 m^2K/W reduced $E_{\%,eff}$ by 20%. For cases where critical layer conditions are reached, the maximum thermal performance equation as is given in equation (6) need to be adjusted to incorporate the influences of thermal interfacial resistances, R_{int} and R_{ext}, thermal conductivities, k_M and k_C, and dimension $\mathcal{Z}$. When critical layering conditions are however not reaches, additional geometric influences are required to determine $E_{\%,eff}$. Due to length restrictions the description of these dependencies fall beyond the scope of this paper.

CONCLUSION

Numerical results indicate that the presence of embedded cooling layers can dramatically increase the ability of a heat-generating medium to accommodate even higher heat-generating densities while maintaining lower steady state peak temperatures. It was found that for configurations with a single directional heat extraction boundary conditions with negligibly small internal and external interfacial thermal resistances, the thermal performance of an embedded cooling layer scheme is dependent upon the thermal conductivities of the cooling and heat-generating materials, the y-directional centre-to-centre offset distances between cooling layers, cooling layer thickness and the z directional dimension of the rectangular heat-generating component.

The influences of these five parameters can be described with three non-dimensional variables namely the volume fraction occupied by cooling, the thermal conductivity ratio of materials in the heat-generating and cooling layers, and the geometric slenderness ratio of the region between two adjacent cooling layers. Equations and Figures were developed with which the achievable thermal performance increase can be determined for a wide range of values for these variables. When thermal interfacial resistance is however present lower thermal performance from a layered structure can be expected.

REFERENCES

[1] Van Wyk J.D., Strydom J.T., Zhao L., and Chen R., Review of the development of high density integrated technology for electromagnetic power passives, *Proceedings of the 2nd International Conference on Integrated Power Systems (CIPS)*, 2002, pp. 25-34

[2] Strydom, J.T., and Van Wyk, J.D., Electromagnetic design optimisation of planar integreted passive modules, *Proceedings of the 33rd I.E.E.E. Power Electronics Specialist Conference (PESC)*, Australia, Vol. 2, June 2002, pp. 573-578

[3] Strydom, J.T., Van Wyk, J.D., and Ferreira, J.A., Some units of integrated L-C-T modules at 1MHz, *I.E.E.E Transactions on Industry Applications*, Vol. 37, No. 3, May/June 2001, pp. 820-828

[4] Dirker, J., Liu, W., Van Wyk, J.D., Meyer, J.P., and Malan, A.G., Embedded solid state heat extraction in integrated power electronic modules, Accepted for publication in the *I.E.E.E. Transactions on Power Electronics*, vol. 20, No. 3, May 2005.

[5] Almogbel M., and Bejan A., Conduction trees with spacing at tips, *International Journal of Heat and Mass Transfer*, Vol. 42, 1999, pp. 3739-3756

[6] Bejan A., and Almogbel M., Constructal T-shaped fins, *International Journal of Heat and Mass Transfer*, Vol. 43, 2000, pp. 2101-2115

[7] Almogbel M., and Bejan A., Cylindrical trees of pin fins, *International Journal of Heat and Mass Transfer*, Vol. 43, 2000, pp. 4285-4297

[8] Bejan A., Constructal-theory networks of conducting paths for cooling a heat generating volume, *International Journal of Heat and Mass Transfer*, Vol. 40, 1997, pp. 799-816

[9] Dirker J., Malan A.G., and Meyer J.P., Numerical modeling and characterization of the thermal behavior of embedded rectangular cooling inserts in modern heat generating mediums, *Proceedings of the 3rd International Conference on Heat Transfer. Fluid Mechanics, and Thermodynamics*, Cape Town, South Africa, Paper DJ1, June 2004.

[10] Dirker J, Liu W, Van Wyk, J.D., and Meyer J.P., Evaluation of embedded heat extraction for high power density integrated electromagnetic passives, *Proceedings of the 35th I.E.E.E. Power Electronics Specialist conference*, Aachen, Germany, Paper number 11430, 21-25 June, 2004.